Influence of Processing Parameters on the Microhardness Property of Laser Cladded Titanium Powder

Influence of Processing Parameters on the Microhardness Property of Laser Cladded Titanium Powder

V.I. Aladesanmi [1*], S.O. Fatoba [1], E.T. Akinlabi[1]

[1]Mechanical Engineering Science Department, University of Johannesburg, South Africa.
Corresponding Author; victorwins03@gmail.com

Abstract-
Laser cladding techniques of additive manufacturing has been globally embraced in the most efficient means of maintenance of steel rail. Nano-composite of titanium has been used as covering layer. The processing parameters of the laser power was varied between 1.0 kW and 2.0 kW while the scanning speed, powder and gas flow rate were kept at constant. Design expert 11 software environment was used to analyze the results derived with a full factorial experiment design guide. The microhardness profiling was performed at a load of 500 g and at a dwelling time of 15 s with the microhardness indenter 20 μm distance was maintained between indentations. An almost uniform weight of Titanium powder was cladded at different variation of processing parameters. A predictive microhardness equation was generated and termss runs intercept of an orthogonal shape. The model terms were found to be significant with logical relationships. It was found that the microhardness increases as the laser power increased.

Key words; factorial experiment, laser cladding, microhardness, nano-composite, steel rail,

1. Introduction

Titanium has been widely used as an anti-corrosive protective layer on common metals like steel[1–3]. Its relatively low density and light weight has made it preferable to steel though more expensive[4]. Steel is widely used due to its availability and affordability but not most-suitable in sea water environment [5–9]. A protective coat layer of manufacturing techniques has been embraced of additive manufacturing in mediums of railway [6,10–12] engineering, ship making, and industrial plants on steel surface. Laser cladding is an additive manufacturing techniques [13–16] that insulates powder metal on a metal plate surface at specified process parameter. Additive Manufacturing through a computerized design helps to store data information for the loading of powder metal layer by layer by feeding the Titanium powder into the melt pool on the substrate[16–18]. This manufacturing techniques can also be used in maintenance of degrading steel rail and other engineering gadgets[19][20]. This experiment varied the laser power of the titanium powder deposition on the steel rail while the scanning speed were kept constant. A factorial design of experiment (DOE) was conducted for an inferential statistical analysis of the results obtained in the study [16][21]. The Design Expert 11 software was used to model the experiments. This is a mathematical statistical design that provides varying range at optimized data performance runs. The results obtained were analyzed and discussed.

2. Methodology

The steel rail substrate 90 × 90 × 20 mm plate was supplied by Transnet South Africa and the Ti powder used is also 99.7 % pure. The steel rail plate was sandblasting and washed with acetone. The laser clad execution entails a Kuka robot with an Nd- YaG laser head and an end effector co-axial powder nozzle guided in a glove box. This delivers the titanium powder into the melt pool process envelope on the surface of the steel substrate and a solid track of laser cladded metal is formed. The scanning speed and scanning rate were kept constant while the laser power utilized was between 1.0 KW and 2.0 KW. The argon gas flow was 2 L/min while the powder flow rate was 2 g/min. A factorial experimental design was made with the Design Expert 11 CAD. The laser cladded sample was latter cut for metallographic investigation. Kroll reagent was used to etch it and later polished. The scanning electron microstructure of the samples were examined. The microhardness was carried out at a load of 500 g and dwell time of 15 secs.

3. Result and discussions

The steel substrate and the Titanium clad surface microstructure were metallurgically analyzed. The steel substrate shows a pearlite and ferrite phase as shown in Fig 1. The morphological structure of the Titanium powder is spherical shaped as shown in Fig 2.

The obtained results were methodically examined in the Design Expert 11 CAD. Table 1 shows the processing parameters as predicted by the DOE of the software of twelve runs. The ANOVA, Co-efficient of determinants, Estimates of determinants and microhardness equation generated are stated bellow. Table 2 reveals the microhardness response results after predictions of varying parameters range.

Table 1; Processing Parameters as Predicted by DOE

		Factor1	Factor2	Response1
Std	Run	A: Laser Power	B: Powder Weight	R1
1	2	1000	28	
2	3	2000	28	
3	10	1250	33	
4	12	1750	33	
5	8	800	30.5	
6	1	2200	30.5	
7	9	1600	269.65	
8	4	1500	340.36	
9	5	1500	30.5	
10	11	1500	30.5	
11	7	1500	30.5	
12	6	1500	30.5	

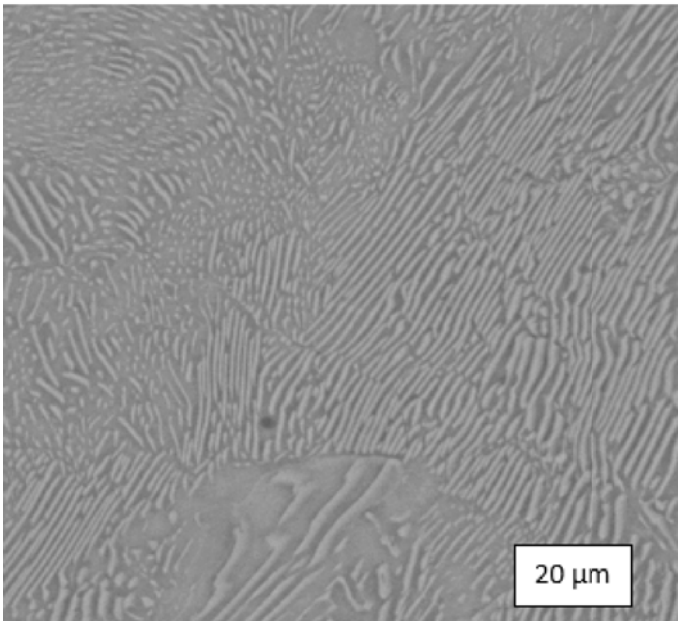

Fig 1; Micrograph of Steel Substrate.

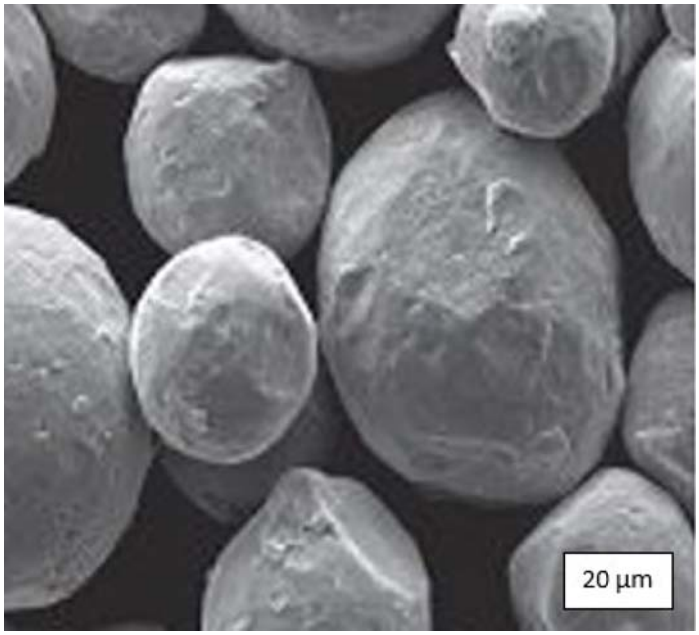

Fig 2; Micrograph of Titanium Powder.

Table 2; Processing Parameter with Microhardness Result.

		Factor1	Factor 2	Response1
Std	Run	A:Laser Power	B:Powder Weight	R1
1	2	1000	28	348.42
2	3	2000	28	672.04
3	10	1250	33	558.14
4	12	1750	33	597.56
5	8	800	30.5	303.14
6	1	2200	30.5	704.12
7	9	1600	269.65	560
8	4	1500	340.36	580
9	5	1500	30.5	574
10	11	1500	30.5	570
11	7	1500	30.5	560
12	6	1500	30.5	550

Table 3; The Analysis of Variance Table (ANOVA)

Source	Sum of Squares	df	Mean Square	F-value	p-value	
Model	1,42E+8	5	28417.9	68.4	< 0.0001	Signi ficant
A-Laser Power	94521.1	1	94521.1	227.5	< 0.0001	
B-Powder Weight	3427.9	1	3427.9	8.5	0.0284	
AB	3986.8	1	3986.8	9.6	0.0212	
A²	5061.3	1	5061.3	12.2	0.0130	
B²	140.1	1	140.1	0.4	0.5826	
Residual	2493.4	6	415.6			
Pure Error	347.0	3	115.7			
Cor Total	1,45E+8	11				

The analysis of variance table was generated and analyzed as shown in Table 3. The model is significant with F-value of 68.38. There is large 0.01% chance that is Factorial-value due to noise. Prob-values less than 0.0500 indicate model terms are significant while value more than 0.1000 are not significant. Our test A, B, AB, A^2 and B^2 are significant model terms

Table 4; Coefficient Determinant

Std. Dev.	20.39	**R^2**	0.9828
Mean	548.12	**Adjusted R^2**	0.9684
C.V. %	3.72	**Predicted R^2**	0.8525
		Adequate Precision	25.4175

Table 4 reveals the coefficient of determinants as generated. The predicted R^2 of 0.8525 is in clear logical accordance with the adjusted R^2 of 0.9684; which means the contrast is less than 0.2. Adequate-Precision calculates the signal to noise ratio. Our ratio of 25.418 indicates an adequate signal.

Table 5; Estimates of Determinants

Factor	**Coefficient Estimate**	**df**	**Standard Error**	**95% CI Low**	**95% CI High**	**VIF**
Intercept	564.3	1	10.0	539.7	588.8	
A-Laser Power	130.9	1	8.7	109.6	152.1	1.2
B-Powder Weight	21.4	1	7.4	3.2	39.5	1.1
AB	-42.9	1	13.8	-76.7	-9.0	1.2
A^2	-30.1	1	8.6	-51.3	-9.0	1.1
B^2	-4.8	1	8.2	-24.9s	15.4	1.0

Table 5 shows the estimates of determinants. The coefficient estimate constitutes the difference in response of terms and change in factor value when all other factors are at constant. The overall response of all the runs is an orthogonal design of the intercepts.

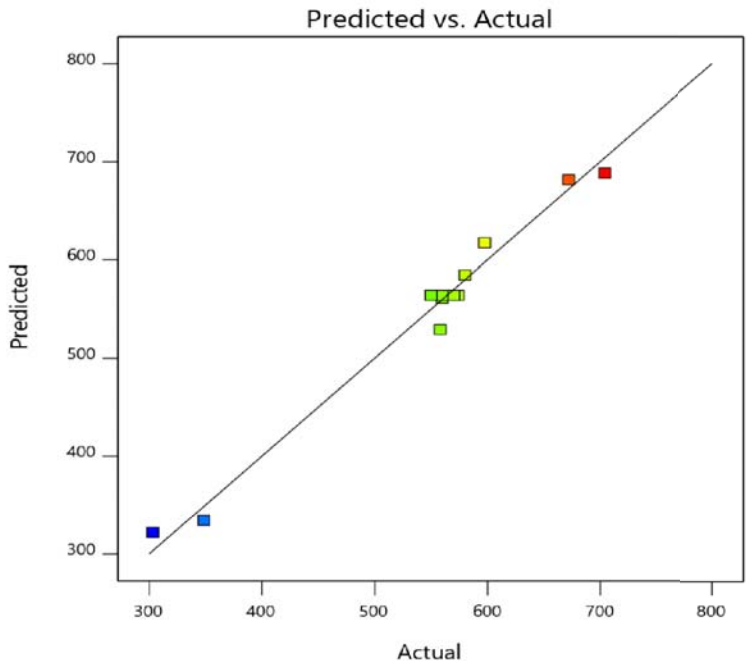

Fig 3; Graph of Predicted against the actual experimental data

Fig 3 shows the graph of predicted microhardness versus the actual experimental microhardness data. Fig 4 & 5 shows the graphical analysis of their residual response. The residuals results are found to be desirable as they are randomly distributed.

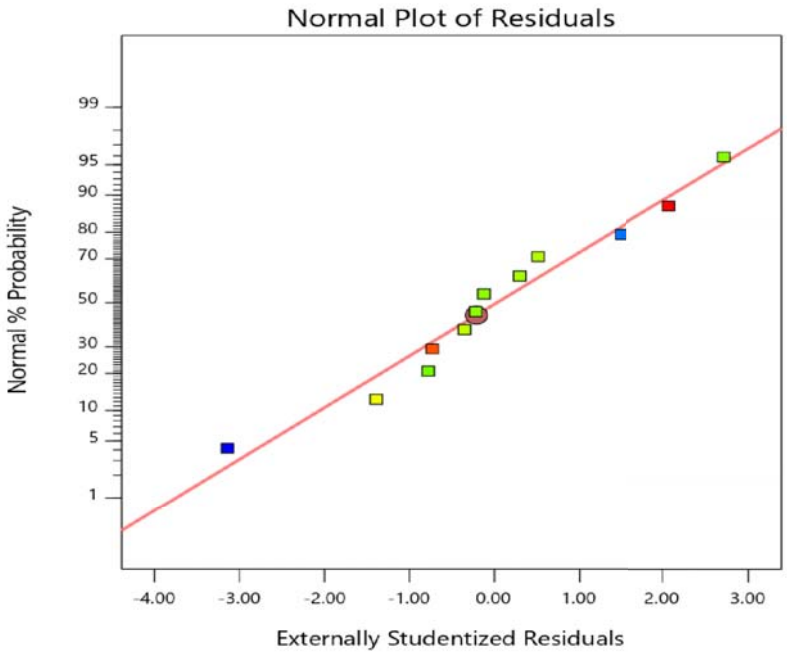

Fig 4; Graph of Normal plot of the residuals

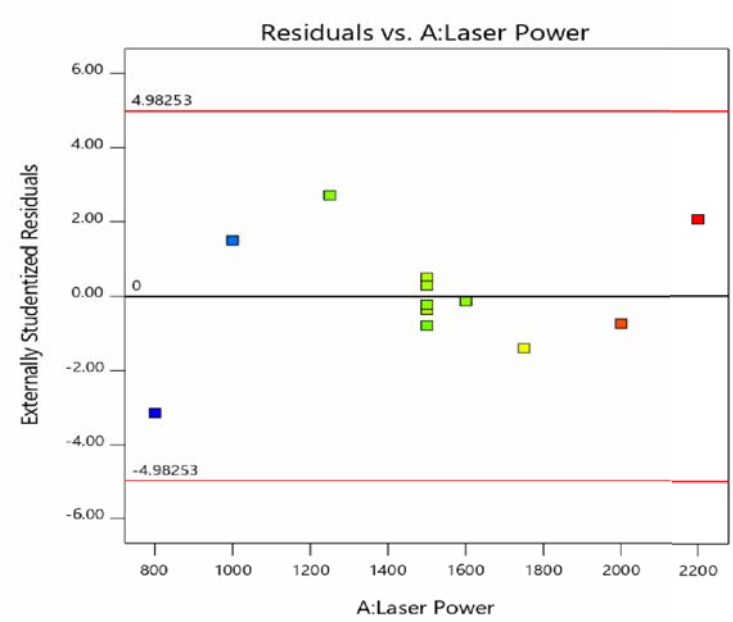

Fig 5; Graph of Residual vs Laser Power

The final computational equation for microhardness is given bellow.

$$R1 = + 564.33 + 130.85 * A + 21.35 * B - 42.86 *AB - 30.13 *A^2 - 4.78 * B^2 \ldots\ldots\ldots (1)$$

Where R1 is the microhardness, A is the Laser Power and B is the Powder Weight. The generated computational equation code factors relationships can be used to predicts response of one another at any given value.

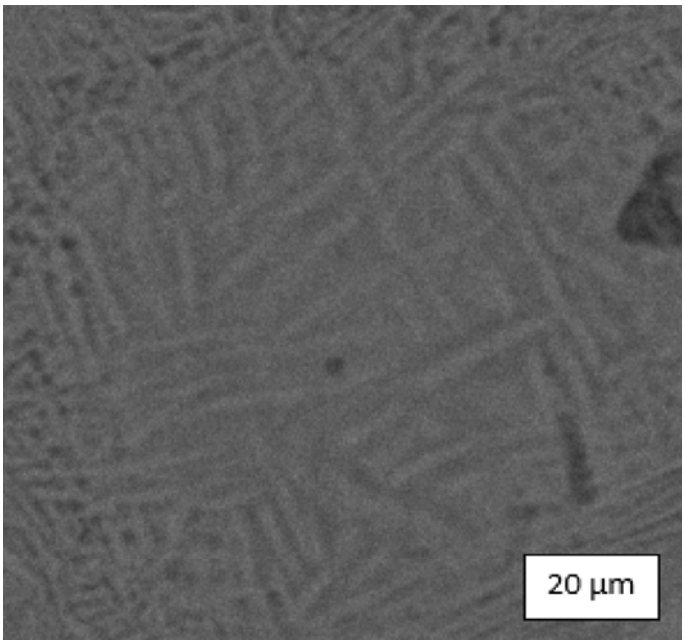

Fig 5; Micrograph of Ti Clad @ 1000 Laser Power

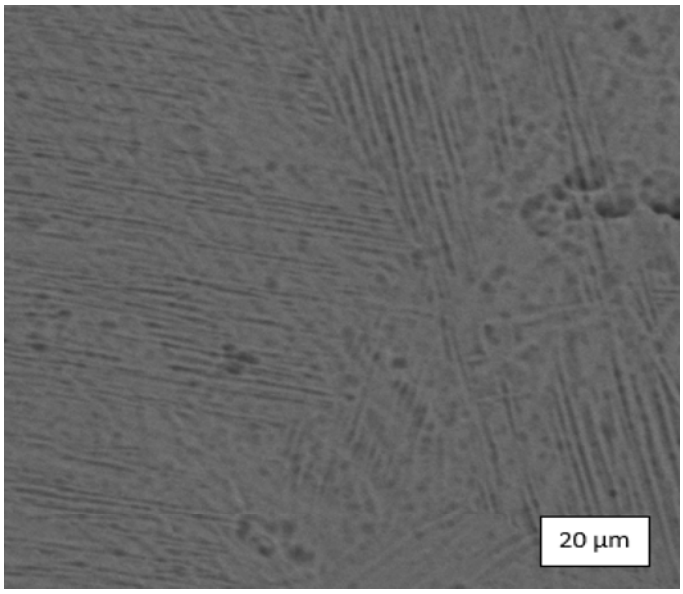

Fig 6; Micrograph of Ti Clad @ 1500 Laser Power

The SEM micrograph of the cladded samples was taken at the laser power of 1KW, 1.5KW and 2.0KW in Fig 5, 6 & 7 respectively.
Fig 5 & 6 shows a Widmastätten microstructure with a low microhardness. It was observed that as the laser power increases, the microhardness increased. The lower the laser power the smaller the melt pool produced which causes a quick solidification of clad. Fig 7 shows a martensitic alpha microstructure with higher hardness. The higher the laser power, the larger the melt pool which creates a larger time of solidification and a higher microhardness.

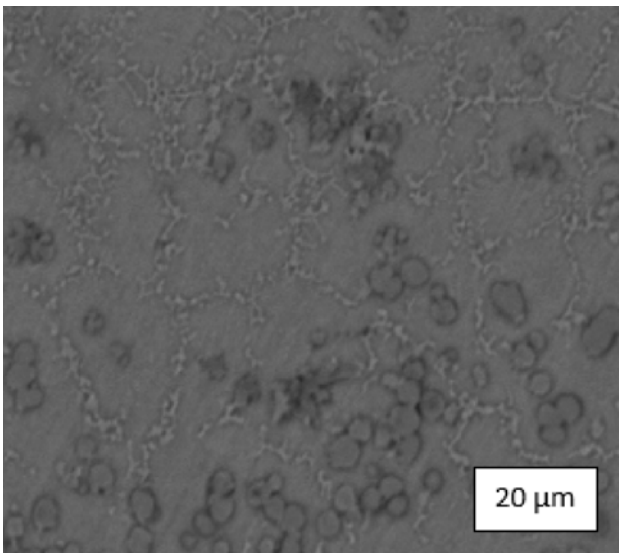

Fig 7; Micrograph of Ti Clad @ 2 000 Laser Power

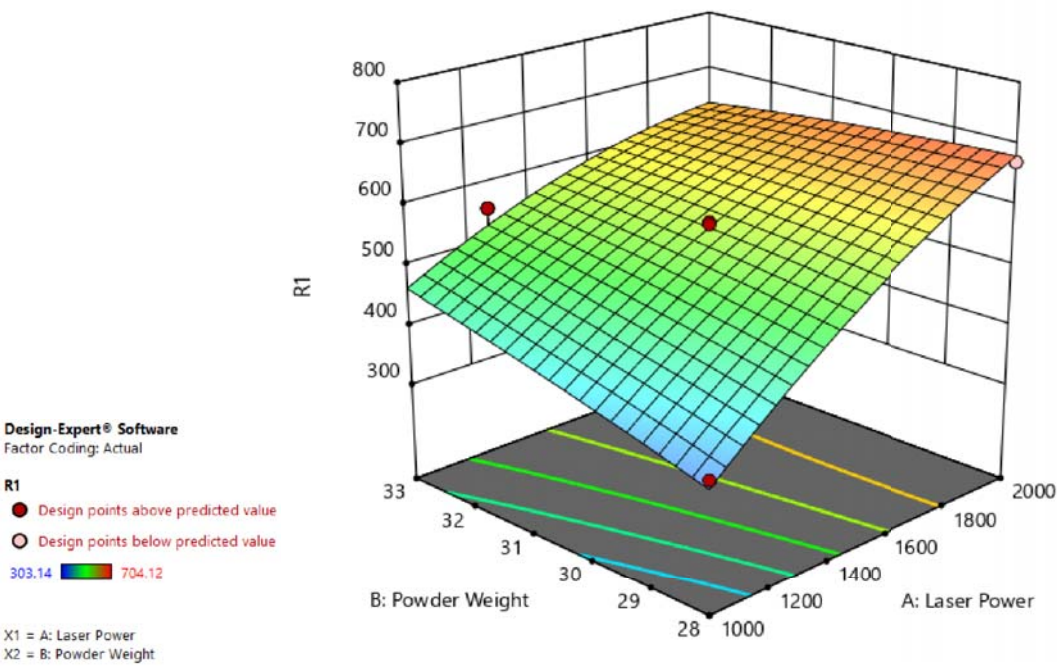

Fig 10; 3D view of the Relative Microhardness with the Laser Power.

The three-dimensional view in Fig 10 shows the surface plot of the microhardness against the laser power at constant scanning, speed and powder flow rate as the powder weight is almost uniform.

4. Conclusion

This paper examined the effect of laser power on the microhardness of laser cladded Titanium. The laser power was varied between 1.0 and 2.0 KW. The results were compiled and examined with the design expert 11 CAD. The model was found to be significant. An orthorhombic shape of intercepts of terms were gotten and the Coefficient of Determinants have logical relationships. A predictive computational equation of microhardness was generated. The study revealed the influence of processing parameter that as the laser power increased, the microhardness also increases. These results reveal the effect of microhardness impact between steel substrate and Titanium powder laser cladding within the range experimented.

Acknowledgement

Authors acknowledged Transnet South Africa, Science4Development Research & Teaching Initiative, Tubingen Germany and National Laser Centre Pretoria, South Africa**.**

Reference

[1] Gao, Q., Yan, H., Qin, Y., Zhang, P., Guo, J. and Chen, Z. (2019) Laser cladding Ti-Ni / TiN / TiW + TiS / WS 2 self-lubricating wear resistant composite coating on Ti-6Al-4V alloy. *Optics and Laser Technology*, Elsevier Ltd. **113**, 182–91. https://doi.org/10.1016/j.optlastec.2018.12.046

[2] Perks, C. and Mudd, G. (2019) Titanium , zirconium resources and production : A state

of the art literature review. *Ore Geology Reviews*, Elsevier. **107**, 629–46. https://doi.org/10.1016/j.oregeorev.2019.02.025

[3] Aladesanmi, V., Fatoba, O. and Akinlabi, E. (2019) Laser cladded Ti + TiB2 on Steel Rail Microstructural Effect. *Procedia Manufacturing*, Elsevier B.V. **33**, 709–16. https://doi.org/10.1016/j.promfg.2019.04.089

[4] Yang, G., Xu, B., Lei, X., Wan, H. and Yang, B. (2018) Preparation of porous titanium by direct in-situ reduction of titanium sesquioxide. *Vacuum*, Elsevier. **157**, 453–7. https://doi.org/10.1016/j.vacuum.2018.09.021

[5] Hasan, S.M., Chakrabarti, D. and Singh, S.B. (2018) Dry rolling/sliding wear behaviour of pearlitic rail and newly developed carbide-free bainitic rail steels. *Wear*, **408**–**409**. https://doi.org/10.1016/j.wear.2018.05.006

[6] Christodoulou, P.I., Kermanidis, A.T. and Haidemenopoulos, G.N. (2016) Fatigue and fracture behavior of pearlitic Grade 900A steel used in railway applications. *Theoretical and Applied Fracture Mechanics*, **83**, 51–9. https://doi.org/10.1016/j.tafmec.2015.12.017

[7] Ueda, M., Uchino, K. and Kobayashi, A. (2002) Effects of carbon content on wear property in pearlitic steels. *Wear*, **253**, 107–13. https://doi.org/10.1016/S0043-1648(02)00089-3

[8] Aladesanmi, V.I., De koker, J. and Myembwe, D. (2016) Material and Wear Characterisation of steel rail on Curved Railway Track. University of Johannesburg, Johannesburg, South Africa.

[9] Jun, H.K., Lee, D.H. and Kim, D.S. (2015) Calculation of minimum crack size for growth under rolling contact between wheel and rail. *Wear*, **344**–**345**, 46–57. https://doi.org/10.1016/j.wear.2015.10.013

[10] Magel, E., Mutton, P., Ekberg, A. and Kapoor, A. (2016) Rolling contact fatigue, wear and broken rail derailments. *Wear*, Elsevier. **366**–**367**, 249–57. https://doi.org/10.1016/j.wear.2016.06.009

[11] Alwahdi, F.A.M., Kapoor, A. and Franklin, F.J. (2013) Subsurface microstructural analysis and mechanical properties of pearlitic rail steels in service. *Wear*, Elsevier. **302**, 1453–60. https://doi.org/10.1016/j.wear.2012.12.058

[12] Seo, J.W., Jun, H.K., Kwon, S.J. and Lee, D.H. (2016) Rolling contact fatigue and wear of two different rail steels under rolling-sliding contact. *International Journal of Fatigue*, Elsevier Ltd. **83**, 184–94. https://doi.org/10.1016/j.ijfatigue.2015.10.012

[13] Zhang, Z. and Kovacevic, R. (2019) Laser cladding of iron-based erosion resistant metal matrix composites. *Journal of Manufacturing Processes*, Elsevier. **38**, 63–75. https://doi.org/10.1016/j.jmapro.2019.01.001

[14] Lu, M., Mccormick, P., Zhao, Y., Fan, Z. and Huang, H. (2018) Laser deposition of compositionally graded titanium oxide on Ti6Al4V alloy. *Ceramics International*, Elsevier Ltd and Techna Group S.r.l. **44**, 20851–61. https://doi.org/10.1016/j.ceramint.2018.08.090

[15] Weng, F., Chen, C. and Yu, H. (2014) Research status of laser cladding on titanium and its alloys : A review. *JOURNAL OF MATERIALS&DESIGN*, Elsevier Ltd. **58**, 412–25. https://doi.org/10.1016/j.matdes.2014.01.077

[16] Dutta, J., Katharina, S., Wissenbach, K., Höche, D., Blawert, C. and Weisheit, A. (2018) Direct laser cladding of the silicide dispersed titanium aluminide. *Optics and Laser Technology*, Elsevier Ltd. **106**, 182–90.

https://doi.org/10.1016/j.optlastec.2018.03.012
[17] Krinitcyn, M., Pribytkov, G., Korzhova, V. and Firsina, I. (2019) Surface & Coatings Technology Structure and properties of composite coatings prepared by electron beam melting with " titanium carbide - titanium binder ." *Surface & Coatings Technology*, Elsevier. **358**, 706–14. https://doi.org/10.1016/j.surfcoat.2018.12.001
[18] Li, X., Zhang, C.H., Zhang, S., Wu, C.L., Liu, Y., Zhang, J.B. et al. (2019) Manufacturing of Ti 3 SiC 2 lubricated Co-based alloy coatings using laser cladding technology. **114**, 209–15. https://doi.org/10.1016/j.optlastec.2019.02.001
[19] Liu, F., Mao, Y., Lin, X., Zhou, B. and Qian, T. (2016) Optics & Laser Technology Microstructure and high temperature oxidation resistance of Ti-Ni gradient coating on TA2 titanium alloy fabricated by laser cladding. *Optics and Laser Technology*, Elsevier. **83**, 140–7. https://doi.org/10.1016/j.optlastec.2016.04.005
[20] Naghiyan, M., Shoja-razavi, R., Allah, H. and Jamali, H. (2018) Surface & Coatings Technology Microstructure investigation of Inconel 625 coating obtained by laser cladding and TIG cladding methods. *Surface & Coatings Technology*, Elsevier. **353**, 25–31. https://doi.org/10.1016/j.surfcoat.2018.08.061
[21] Juan, Y.F., Li, J., Jiang, Y.Q., Jia, W.L. and Lu, Z.J. (2019) Applied Surface Science Modified criterions for phase prediction in the multi-component laser-clad coatings and investigations into microstructural evolution / wear resistance of FeCrCoNiAlMox laser-clad coatings. **465**, 700–14. https://doi.org/10.1016/j.apsusc.2018.08.264